



**Universiteit  
Leiden**  
The Netherlands

## **Comparative analysis of spike-specific IgG Fc glycoprofiles elicited by adenoviral, mRNA, and protein-based SARS-CoV-2 vaccines**

Coillie, J. van; Pongracz, T.; Sustic, T.; Wang, W.J.; Nouta, J.; Gars, M. le; ... ; COUGH1 Study Grp

### **Citation**

Coillie, J. van, Pongracz, T., Sustic, T., Wang, W. J., Nouta, J., Gars, M. le, ... Vidarsson, G. (2023). Comparative analysis of spike-specific IgG Fc glycoprofiles elicited by adenoviral, mRNA, and protein-based SARS-CoV-2 vaccines. *Isience*, 26(9).  
doi:10.1016/j.isci.2023.107619

Version: Publisher's Version

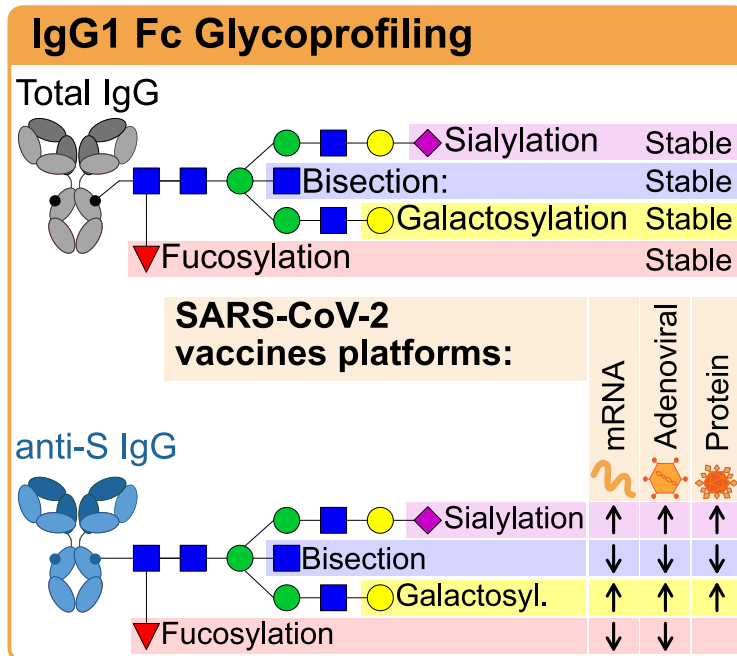
License: [Creative Commons CC BY-NC-ND 4.0 license](#)

Downloaded from: <https://hdl.handle.net/1887/3754672>

**Note:** To cite this publication please use the final published version (if applicable).

Article

# Comparative analysis of spike-specific IgG Fc glycoprofiles elicited by adenoviral, mRNA, and protein-based SARS-CoV-2 vaccines



Julie Van Coillie, Tamas Pongracz, Tonći Šuštić, ..., in collaboration with the UMC COVID-19 S3/HCW study group, Fatebenefratelli-Sacco Infectious Diseases Physicians group, Radboud University Medical Center (RUMC) and COUGH1 study group

[g.vidarsson@sanquin.nl](mailto:g.vidarsson@sanquin.nl)

**Highlights**

Vaccine-induced anti-S IgG1 Fc glycosylation is dynamic regardless of the vaccine used

Similar anti-S IgG1-Fc glycoprofiles are observed for different vaccine platforms

Transient IgG1-Fc afucosylation is strongest for mRNA and adenoviral vaccines

Functional FcγRIIIa-based immunoassay corroborates LC-MS obtained data

Van Coillie et al., iScience 26, 107619  
September 15, 2023 © 2023 The Author(s).  
<https://doi.org/10.1016/j.isci.2023.107619>



## Article

## Comparative analysis of spike-specific IgG Fc glycoprofiles elicited by adenoviral, mRNA, and protein-based SARS-CoV-2 vaccines

Julie Van Coillie,<sup>1,2,12</sup> Tamas Pongracz,<sup>3,12</sup> Tonći Šuštić,<sup>1,2</sup> Wenjun Wang,<sup>3</sup> Jan Nouta,<sup>3</sup> Mathieu Le Gars,<sup>4</sup> Sofie Keijzer,<sup>5</sup> Federica Linty,<sup>1,2</sup> Olvi Cristianawati,<sup>5</sup> Jim B.D. Keijser,<sup>5</sup> Remco Visser,<sup>1,2</sup> Lonneke A. van Vught,<sup>6,7</sup> Marleen A. Slim,<sup>6,7</sup> Niels van Mourik,<sup>6,7</sup> Merel J. Smit,<sup>8</sup> Adam Sander,<sup>9,10</sup> David E. Schmidt,<sup>1</sup> Maurice Steenhuis,<sup>5</sup> Theo Rispens,<sup>5</sup> Morten A. Nielsen,<sup>9</sup> Benjamin G. Mordmüller,<sup>8</sup> Alexander P.J. Vlaar,<sup>7,11</sup> C. Ellen van der Schoot,<sup>1</sup> Ramon Roozendaal,<sup>4</sup> Manfred Wuhrer,<sup>3</sup> Gestur Vidarsson,<sup>1,2,13,\*</sup> and in collaboration with the UMC COVID-19 S3/HCW study group, Fatebenefratelli-Sacco Infectious Diseases Physicians group, Radboud University Medical Center (RUMC) and COUGH1 study group

## SUMMARY

**IgG antibodies are important mediators of vaccine-induced immunity through complement- and Fc receptor-dependent effector functions. Both are influenced by the composition of the conserved N-linked glycan located in the IgG Fc domain. Here, we compared the anti-Spike (S) IgG1 Fc glycosylation profiles in response to mRNA, adenoviral, and protein-based COVID-19 vaccines by mass spectrometry (MS). All vaccines induced a transient increase of antigen-specific IgG1 Fc galactosylation and sialylation. An initial, transient increase of afucosylated IgG was induced by membrane-encoding S protein formulations. A fucose-sensitive ELISA for antigen-specific IgG (FEASI) exploiting FcγRIIIa affinity for afucosylated IgG was used as an orthogonal method to confirm the LC-MS-based afucosylation readout. Our data suggest that vaccine-induced anti-S IgG glycosylation is dynamic, and although variation is seen between different vaccine platforms and individuals, the evolution of glycosylation patterns display marked overlaps.**

## INTRODUCTION

SARS-CoV-2 vaccines induce robust IgG responses against the spike protein, particularly IgG1.<sup>1</sup> Spike-specific IgG, induced by viral infection, vaccination, or convalescent plasma treatment,<sup>2–8</sup> can convey protection against SARS-CoV-2 infection and/or COVID-19 progression. While the IgG antigen-binding fragment (Fab) is responsible for neutralization, the crystallizable fragment (Fc) domain extends the half-life via increased FcRn-binding<sup>9</sup> and affects optimal protection through classical FcγR or complement binding.<sup>10</sup> Importantly, the IgG Fc N-glycans play a major role in fine-tuning these latter Fc-effector functions.<sup>11</sup> The conserved N-glycan at position N297 consists of a biantennary glycan with a pentasaccharide core that can be further elongated by the addition of bisecting N-acetylglucosamine (GlcNAc), fucose, galactoses, and sialic acids (Figure 1).

While most human IgG is fucosylated (~94% of total IgG), IgG lacking core fucose (afucosylated IgG) is found against allo-antigens on blood cells,<sup>14–16</sup> antigens of *Plasmodium falciparum* expressed on the red blood cell (RBC) membrane,<sup>17</sup> and various enveloped viruses,<sup>18–21</sup> as recently reviewed by Oosterhoff et al.<sup>11</sup> Interestingly, a common denominator of these responses is host cell membrane-embedded antigen recognition. Afucosylated IgG has an increased affinity (up to 40 times) to the FcγRIII receptor family, enhancing activation of myeloid and NK cells, and subsequent antibody-dependent cellular cytotoxicity (ADCC).<sup>22–24</sup> In addition, targets opsonized with afucosylated IgG are more capable of inducing

<sup>1</sup>Department of Experimental Immunohematology, Sanquin Research, Amsterdam, the Netherlands

<sup>2</sup>Department of Biomolecular Mass Spectrometry and Proteomics, Utrecht Institute for Pharmaceutical Sciences and Bijvoet Center for Biomolecular Research, Utrecht University, Utrecht, the Netherlands

<sup>3</sup>Center for Proteomics and Metabolomics, Leiden University Medical Center, Leiden, the Netherlands

<sup>4</sup>Janssen Vaccines & Prevention B.V., Leiden, the Netherlands

<sup>5</sup>Department of Immunopathology, Sanquin Research, Amsterdam, the Netherlands

<sup>6</sup>Center for Experimental and Molecular Medicine, Amsterdam Infection & Immunity Institute, Amsterdam, the Netherlands

<sup>7</sup>Department of Intensive Care, Amsterdam University Medical Center, University of Amsterdam, Amsterdam, the Netherlands

<sup>8</sup>Department of Medical Microbiology, Radboudumc Center for Infectious Diseases, Radboud University Medical Center, Nijmegen, the Netherlands

<sup>9</sup>Centre for Medical Parasitology, Department for Immunology and Microbiology, Faculty of Health and Medical Sciences, University of Copenhagen, Copenhagen, Denmark

<sup>10</sup>AdaptVac Aps, Copenhagen, Denmark

<sup>11</sup>Laboratory of Experimental Intensive Care and Anaesthesiology, L.E.I.C.A., Amsterdam University Medical Center, University of Amsterdam, Amsterdam, the Netherlands

<sup>12</sup>These authors contributed equally

<sup>13</sup>Lead contact

\*Correspondence: g.vidarsson@sanquin.nl

<https://doi.org/10.1016/j.isci.2023.107619>



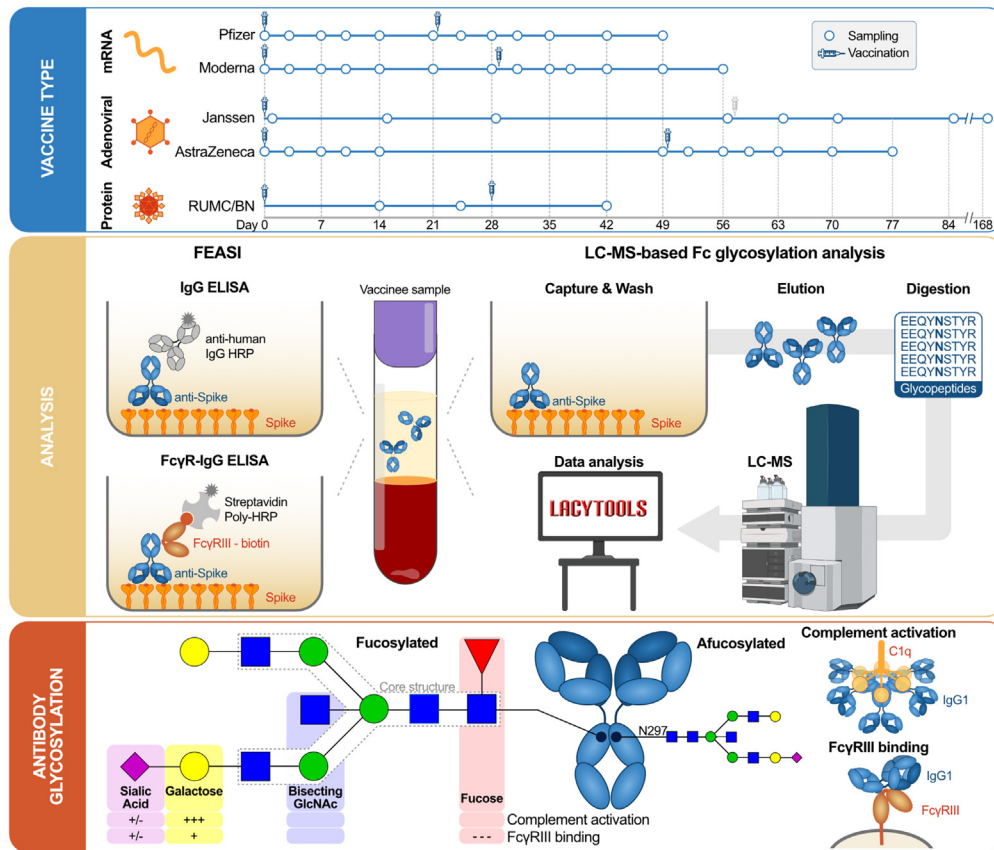


**Figure 1. Workflow of vaccine-induced antibody analysis by LC-MS and FEASI**

Upper panel: Longitudinal sampling regimen of study participants vaccinated with the various vaccine platforms. Middle panel: (left) Fucose-sensitive ELISA for anti-S IgG (FEASI) quantification (IgG ELISA) and Fc $\gamma$ RIII-binding to anti-S specific IgG (Fc $\gamma$ R-IgG ELISA) to determine IgG fucosylation; and (right) anti-S IgG1 glyco-profiling by liquid chromatography-mass spectrometry (LC-MS) by anti-S capture, wash, elution, digestion, LC-MS, and data extraction with LaCyTools.<sup>12,13</sup> Lower panel: Influence of anti-S IgG1 Fc glycosylation traits on complement activation and Fc $\gamma$ RIII binding.

NK cell responses than those with fucose-enriched IgG.<sup>23,25</sup> The fucosylation levels of *de novo* antibodies induced in aforementioned responses varied (5–90%)<sup>11</sup> and were previously thought to be stable over decades, as constant afucosylation levels have been observed for human immunodeficiency virus (HIV),<sup>20</sup> cytomegalovirus (CMV),<sup>18</sup> malaria,<sup>17</sup> RBC,<sup>26</sup> and platelets.<sup>15</sup> More recently, however, transient afucosylated responses have been observed in naive individuals both following SARS-CoV-2 infection<sup>18,27–29</sup> and Pfizer/BioNTech BNT162b2 mRNA vaccination.<sup>12,29,30</sup>

IgG Fc galactosylation levels are highly variable between individuals and decline with age.<sup>31–33</sup> Functionally, increased galactosylation elevates the potential of IgG to activate the classical complement pathway via increased binding to C1q.<sup>23,34</sup> This increase is mediated by the formation of IgG hexamers that serve as docking platforms for the hexameric C1q.<sup>35–38</sup> On top of this, IgG galactosylation slightly enhances the binding to Fc $\gamma$ R, particularly for afucosylated IgG.<sup>23</sup> By contrast, the functional effects of bisection and sialylation of IgG1 Fc portions appear to be minor or negligible.<sup>23,35,39</sup>

Protein and attenuated viral vaccines have been reported to exclusively induce fucosylated antigen-specific IgG<sup>17,40,41</sup> with increased levels of galactosylation and sialylation.<sup>20,40,42</sup> These vaccines are mainly composed of proteins and/or polysaccharides, and in contrast to mRNA and adenovirus-based vaccines, do not result in host membrane embedding of the antigen. We have previously postulated that afucosylated IgG responses are only found against membrane-embedded epitopes<sup>11,18</sup> and recently found that the BNT162b2 mRNA vaccine induces an initial, transient afucosylated response in most naive, but not in SARS-CoV-2 antigen-experienced individuals.<sup>12</sup>

Here, we set out to characterize and compare IgG1 Fc glycosylation in individuals administered with different SARS-CoV-2 vaccine platforms including the mRNA-based Pfizer/BioNTech (BNT162b2) and Moderna (mRNA-1273) vaccines, as well as the adenovirus-based Janssen (Ad26.COV2.S) and AstraZeneca (ChAdOx1nCoV-19) vaccines. We also included the S protein-based capsid virus-like particle (cVLP; ABNCoV2) vaccine.<sup>43</sup> We assessed the vaccine-induced, S protein-specific IgG1 Fc glycosylation by liquid chromatography-mass spectrometry (LC-MS) for all vaccines. In addition, fucosylation was assessed with an immunoassay named fucose-sensitive ELISA for antigen-specific IgG (FEASI).<sup>44</sup> This immunoassay quantifies antigen-specific IgG levels and qualitatively determines IgG responses with an Fc $\gamma$ RIII binding-dependent readout. Vaccination against SARS-CoV-2 resulted in dynamic changes in spike-specific IgG1 fucosylation, galactosylation, and sialylation, which displayed similarities between different vaccine platforms.

**Table 1. Summary of vaccination cohort**

	Pfizer	Moderna	Janssen	AstraZeneca	RUMC/COUGH1
Manufacturer	Pfizer/BioNTech	Moderna	Janssen Vaccines and Prevention	AstraZeneca	AdaptVac & Bavarian Nordic
Trade name	Comirnaty	SpikeVax	JCOVDEN	Vaxzevria	NA
Vaccine name	BNT162b2	mRNA-1273	Ad26.COVS.S	ChAdOx1nCoV-19	ABNCoV2
Vaccine platform	mRNA	mRNA	Adenovector	Adenovector	Protein vaccine Capsid-like particle
<b>Participants</b>					
N	48	8	78	17	45
Of which ag-exp.	6 (15%)	0 (0%)	1 (1%)	2 (12%)	0 (0%)
Positive PCR	5	0	0	2	0
Female, n (%)	32 (67%)	8 (100%)	25 (32%)	13 (76%)	26 (58%)
Male, n (%)	16 (33%)	0 (0%)	53 (68%)	4 (24%)	19 (42%)
<b>Age</b>					
Range	23-64	26-56	20-79	60-66	18-54
Median	40	33	50	62	26
Q1-Q3	32-50	27-44	36-67	61-65	22-34
<b>Regimen</b>					
Different regimens	No	No	2	No	7
Days between doses	20-24	28	57	43-78	26-35
Doses received	2	2	1 or 2	2	2
Serum analysis (days after 1 <sup>st</sup> dose)	0, 3, 7, 10, 14, 21, 24, 28, 31, 35, 42, 49	0, 3, 7, 10, 21, 28, 35, 38, 42, 49, 56	1, 15, 29, 57, 64, 71, 85, 169	0, 3, 7, 10, 14, 21, 28, 77, 80, 84, 87, 91, 98, 105	14, 24, 42

## RESULTS

### Vaccine study cohorts

Vaccine-induced antibody responses were compared across three different SARS-CoV-2 vaccine platforms: mRNA- and adenoviral-based, and a capsid-like protein vaccine (Figure 1A; and Table 1), using the previously characterized Pfizer mRNA cohort (n = 48).<sup>12</sup> We included cohorts vaccinated with the mRNA1273 Moderna vaccine (n = 8), adenoviral-based Ad26.COVS.S Janssen (n = 78) and ChAdOx1nCoV-19 AstraZeneca vaccine (n = 17), and the S protein-based cVLP ABNCoV2 vaccine (n = 45).<sup>43</sup> Vaccinees in these cohorts were sampled longitudinally and received a second dose according to specific regimens (Figure 1A; Tables 1 and S1–S5). Individuals were classified as antigen-experienced according to prior positive PCR tests when available, and/or if anti-S and anti-nucleocapsid (N) levels exceeded pre-outbreak levels prior to vaccination (Figures 1A, 2A, and S1; Tables S1–S5). Formal sample size calculations were not conducted for this current study, nor were individuals included based on demographics, i.e., samples were included based on availability. The different location and timing of sampling resulted in significant differences between cohorts with respect to age (ANOVA,  $p = 3.2 \times 10^{-11}$ ) and sex (Chi-square,  $p = 1.6 \times 10^{-5}$ ) (Table S6). Combined, the cohorts span a range of ages from 18 to 79 years, with a female ratio of 53%.

### All vaccine platforms induce detectable anti-S IgG levels

First, anti-S IgG levels were determined for all vaccine cohorts by ELISA. To determine the pre-outbreak threshold, the anti-S levels were measured in 264 pre-pandemic samples (Figure S2). In line with previous work, detectable anti-S IgG levels for naive vaccinees were measured at the first available time point for these cohorts (between days 7 and 10 for the mRNA vaccines and AstraZeneca, and at days 14 and 15 for RUMC/COUGH1 and Janssen, respectively). The anti-S levels further increased after the second dose (Figures 2A and S4).<sup>1</sup> Vaccinees in the Janssen cohort received either one or two doses, with higher levels of anti-S being observed in individuals receiving two doses (Figures 2A, S3A, and S4).<sup>3,45</sup> Lower anti-S levels were observed in the AstraZeneca cohort in comparison to the mRNA and protein vaccines, as previously described (Figure S4).<sup>46</sup> In the RUMC/COUGH1 vaccine cohort, participants were vaccinated with increasing doses with or without the MF59 adjuvant, both of which generally resulted in increased anti-S IgG levels (Figures 2A and S5A). All antigen-experienced individuals had detectable anti-S levels before vaccination, which increased after the first dose (Figure 2A). Naive individuals receiving two doses reached anti-S IgG levels similar to antigen-experienced vaccinees after one dose. An exception was AstraZeneca, where two antigen-experienced vaccinees exhibited considerably higher levels than most naive individuals receiving two doses (Figure 2A).

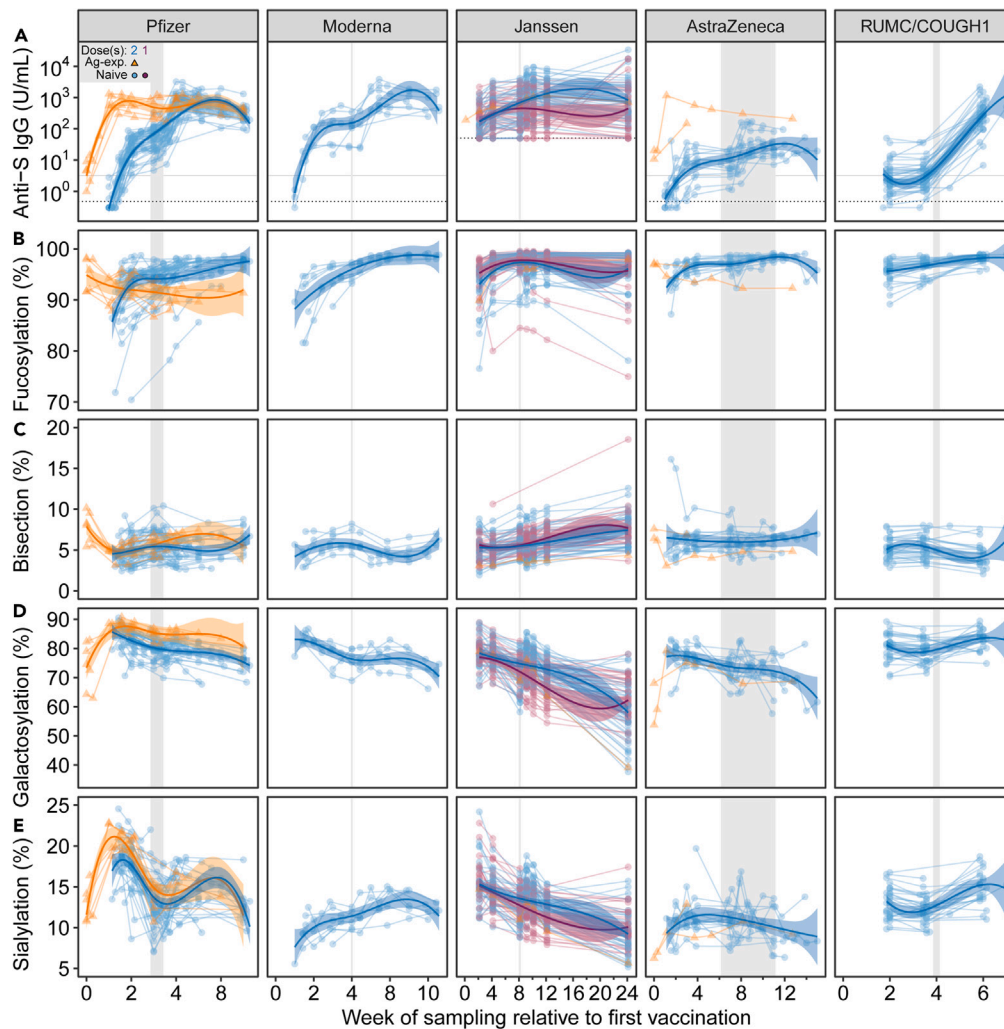


**Figure 2. Dynamics of anti-Spike IgG levels and IgG1 Fc glycosylation**

(A) Longitudinal anti-S IgG levels in Arbitrary Units (AU) per mL for all vaccines except for Janssen, which is expressed in Antibody Binding Units (ABU) per mL (thus not directly comparable with the other cohorts). The dotted horizontal line signifies the limit of detection. The solid horizontal line signifies the pre-outbreak threshold value as determined by pre-pandemic samples (95<sup>th</sup> percentile) (Figure S2). IgG1 Fc (B) fucosylation, (C) bisection, (D) galactosylation, and (E) sialylation for naive (circle, purple: one dose, blue: two doses) and antigen-experienced (orange triangle: two doses) vaccinees for Pfizer (n = 48), Moderna (n = 8), one (n = 39) or two (n = 39) doses Janssen (n = 78), AstraZeneca (n = 17), and RUMC/COUGH1 (n = 45). Range of the scheduled second vaccine dose is depicted vertically in gray. Previously published Pfizer data are included for comparative purposes.<sup>12</sup> Statistical comparisons were conducted between the timepoints 2 weeks after 1<sup>st</sup> and 2 weeks after 2<sup>nd</sup> vaccination dose and are presented in Figures S4 and S6 for anti-S levels and glycosylation traits, respectively.

### Vaccine-induced anti-S IgG1 Fc glycosylation is dynamic

Next, we established the longitudinal anti-S IgG1 Fc glycosylation profiles and compared these across the studied vaccine platforms (Figures 1 and 2B–2E). Sex and age have been reported to influence total IgG glycosylation.<sup>31,32</sup> Indeed, we found that both sex and age affected the total IgG glycosylation profiles, although to a limited extent (Table S7). However, in spite of the differences observed in age in a sex-stratified manner among the cohorts, their influence remains unaffected on the anti-S IgG Fc profiles (Table S8).

Dynamic anti-S IgG1 Fc glycosylation was observed across all cohorts with a substantial variation in responses between individuals (Figures 2B–2E). We previously observed a transient, afucosylated anti-S IgG1 glycosylation pattern in naive, but not antigen-experienced vaccinees for the Pfizer mRNA vaccine.<sup>12</sup> Similarly, an initial, transient afucosylated anti-S IgG response was observed after the first dose, which diminished over time. After 2 weeks, all cohorts reached near fully fucosylated IgG glycosylation profiles (Figures 2B and S6A). The strongest afucosylation levels were observed for individuals in the mRNA and Janssen cohorts. However, early afucosylation levels might have been missed in samples with low IgG levels, especially for AstraZeneca, but also because of lack of very early time points (i.e., before day 14). For some individuals (7 out of 78) in the Janssen cohort, a sustained afucosylation trend was observed after 50 days, regardless of the



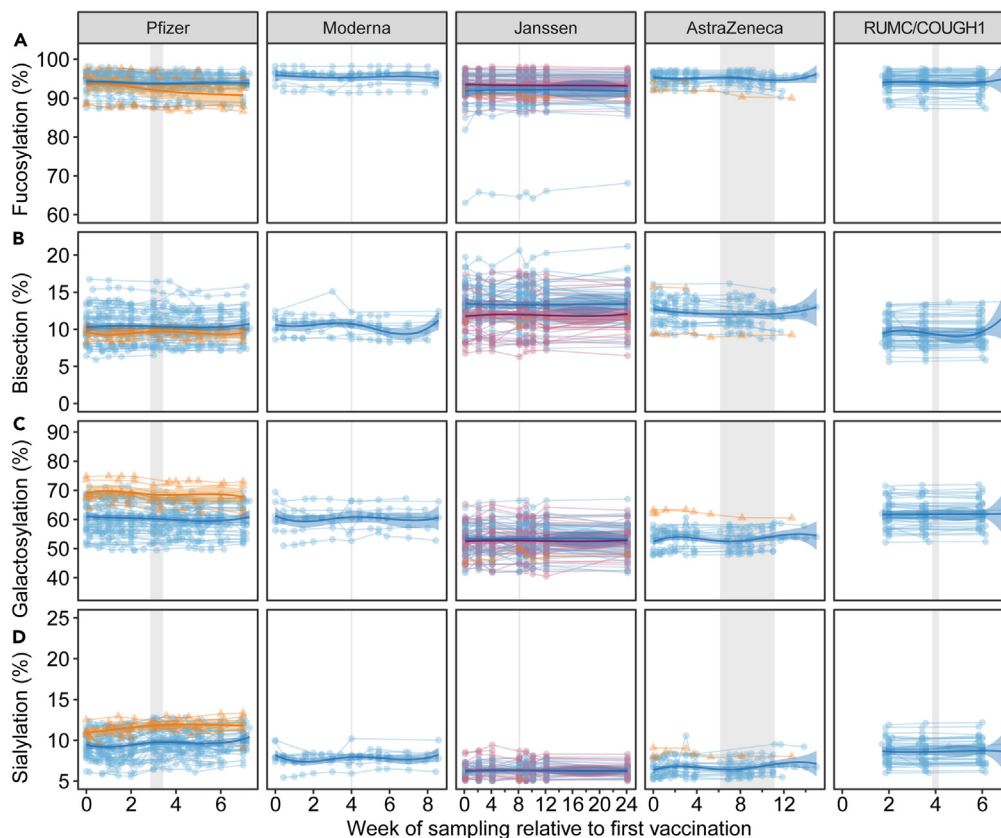


**Figure 3. Total IgG1 Fc glycosylation is stable over time**

Longitudinal, total IgG1 Fc (A) fucosylation, (B) bisection, (C) galactosylation, and (D) sialylation for naive (circle, purple: one dose, blue: two doses) and antigen-experienced (orange triangle: two doses) vaccinees for Pfizer (n = 48), Moderna (n = 8), one (n = 39) or two (n = 39) doses Janssen (n = 78), AstraZeneca (n = 17), and RUMC/COUGH1 (n = 45). Range of the scheduled second vaccine dose is depicted vertically in gray. Previously published data were included for comparative purposes.<sup>12</sup>

number of doses (Figures 2B and S3B). For all vaccine platforms, anti-S IgG1 bisection levels were also dynamic over time, but appeared to be comparable two weeks after the first and second doses (Figures 2C and S6B). Anti-S IgG1 galactosylation and sialylation were highly dynamic across all cohorts. A transient increase of anti-S IgG1 galactosylation and sialylation was observed after the first dose (Figures 2C, 2D, S6C, and S6D). This was also observed after the second dose for the Janssen and RUMC/Bavarian Nordic (BN) cohort (Figures 2C, 2D, S3D, S3E, and S5D–S5E).

### Similar vaccine-induced anti-S Fc glycosylation is observed

Albeit dynamic antigen-specific anti-S IgG1 glycosylation levels were observed, no such changes were observed for total IgG1 Fc glycosylation (Figures 2 and 3).

The initial levels of anti-S IgG1 Fc fucosylation generally reached levels similar or higher to total IgG three to four weeks after the first dose (Figures 2B, 3A, and S8A). For Pfizer, Janssen, and RUMC/COUGH1, anti-S IgG1 bisection levels were significantly lower than their total IgG1 counterpart (Figures 2C, 3B, and S8B). Furthermore, significant increases in anti-S IgG1 Fc galactosylation and sialylation levels were seen observed compared to total IgG1 for these three vaccines (Figures 2D, 2E, 3C, 3D, S8C, and S8D). Similar trends were also seen for both Moderna and AstraZeneca, albeit not significant, likely due to the small sample size of both cohorts (Figures 3 and S8C). In summary, albeit differences in anti-S IgG1 Fc glycosylation levels were seen between individuals and vaccine platforms, similar changes were observed in anti-S compared to total IgG1 Fc glycosylation.

### Anti-S IgG1 fucosylation correlates with FcγRIIIa binding

To assess the functional impact of afucosylation, we measured IgG Fc fucosylation with FEASI. This dual ELISA-based method uses both a typical anti-S IgG ELISA (Figure 2A) and an FcγRIIIa ELISA (FcγRIIIa-IgG ELISA) (Figures 4A and 1, middle panel). The latter uses the sensitivity of FcγRIIIa to IgG fucosylation as a proxy to quantify IgG fucosylation levels (Figures 1 and 4A). This FcγRIIIa binding (Figure 4A) is normalized against the anti-S IgG levels measured (Figure 2A) to quantify a degree of antigen-specific IgG fucosylation (Figure 4B). FEASI was not carried

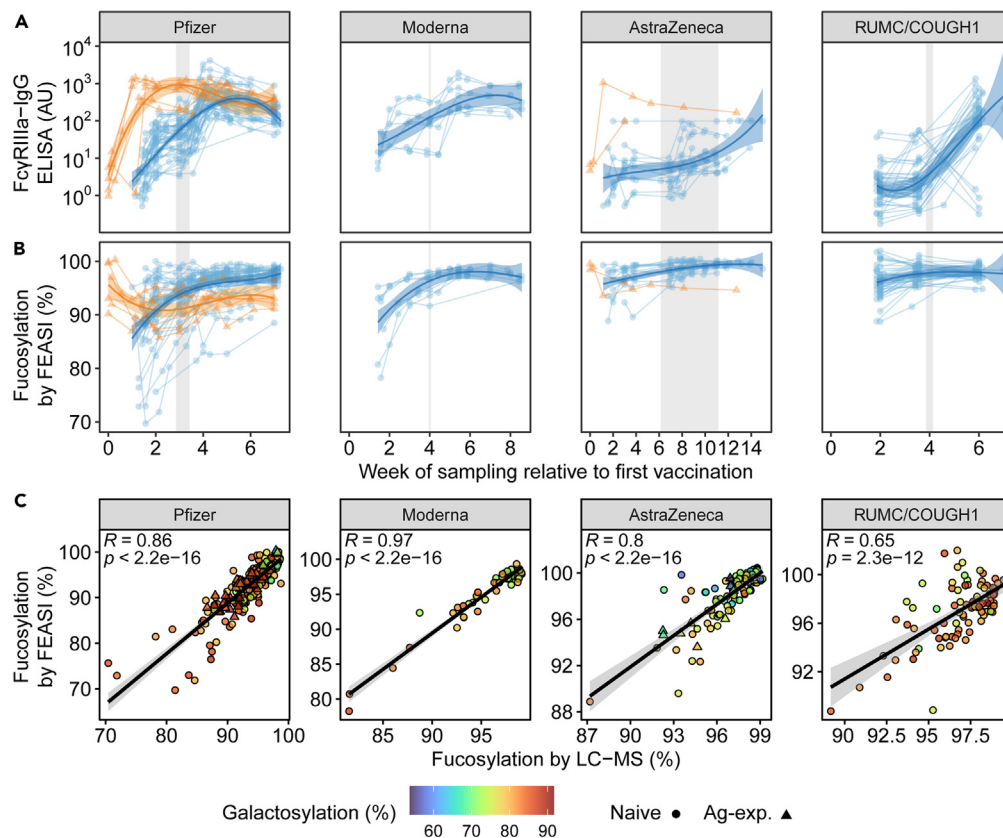


**Figure 4. Anti-Spike IgG1 fucosylation level correlates with Fc $\gamma$ RIIIa binding**

(A) Anti-S IgG binding to Fc $\gamma$ RIIIa.

(B) Anti-S fucosylation levels determined by FEASI for naive (blue circle) and antigen-experienced (orange triangle) vaccinees for Pfizer (n = 39), Moderna (n = 8), AstraZeneca (n = 17), and RUMC/COUGH1 (n = 45).

(C) Spearman's correlation of anti-S IgG fucosylation determined by FEASI and LC-MS for all available time points (circle: naive; triangle: antigen-experienced vaccinees). Color gradient indicates galactosylation level.

out for the Janssen cohort due to sample unavailability. For all other cohorts, dynamic Fc $\gamma$ RIIIa binding was seen over time. Initially, the Fc $\gamma$ RIIIa binding was low due to low anti-S IgG levels. Over time, the Fc $\gamma$ RIIIa binding further increased (Figure 4A). After correcting for anti-S IgG levels (Figure 2A), the FEASI-obtained IgG fucosylation levels (Figure 4B) correlated strongly to the corresponding LC-MS measurement (Figure 4C). As IgG Fc galactosylation has been shown to have a minor enhancing effect on Fc $\gamma$ RIII affinity, in particular on afucosylated IgG,<sup>23,44</sup> the IgG Fc glycosylation levels are depicted by a color gradient (Figure 4C). However, this enhancing effect was not observed in this study on naturally glycovariant IgG as in the aforementioned studies on glycoengineered monoclonal IgG.

## DISCUSSION

Vaccination can potentially influence vaccine-elicited antigen-specific IgG Fc glycosylation, although the mechanisms and consequences remain unclear at present. In this study, we investigated the influence of multiple SARS-CoV-2 vaccine platforms on antigen-specific antibody glycosylation. We utilized LC-MS to longitudinally characterize anti-S IgG1 Fc N-glycosylation for two mRNA vaccines (BNT162b2, Pfizer and mRNA-1273, Moderna), two adenovirus-based vaccines (Ad26.COVS.2, Janssen and ChAdOx1nCoV-19, AstraZeneca), and an S protein-based cVLP vaccine (ABNCoV2, RUMC/COUGH1). We furthermore applied the FEASI immunoassay, utilizing Fc $\gamma$ RIII binding to measure afucosylation levels, which corroborated the LC-MS-obtained fucosylation levels.

Natural SARS-CoV-2 infection induces dynamic, specific anti-S IgG1 Fc glycosylation patterns.<sup>18,27,28,47–49</sup> Notably, remarkably elevated afucosylated anti-spike IgG has been shown to be most prominent at seroconversion in severe COVID-19 patients, which reverted to normal levels within 2–3 weeks for most individuals.<sup>18,28,49,50</sup> The observed afucosylation was associated with increased inflammatory cytokine levels and immune-related pathologies.<sup>18,50</sup> Furthermore, at seroconversion, elevated anti-S and -N IgG1 Fc galactosylation and sialylation and low bisection were found.<sup>18,27,48</sup> However, these high galactosylation and sialylation levels, particularly the former, dropped quickly in the following 2–3 weeks (from ~80% to ~30% for galactosylation).<sup>11,27,48</sup>



Anti-S IgG1 glycosylation upon BNT162b2 mRNA vaccination has also been reported to be highly dynamic.<sup>12,29,51</sup> In this study, we likewise observed dynamic anti-S IgG1 Fc glycosylation responses over time and revealed similar trends for other SARS-CoV-2 vaccine platforms. Upon seroconversion, transient afucosylated anti-S was found in all vaccine platforms, albeit to a lesser extent for AstraZeneca and RUMC/COUGH1. However, early afucosylated responses might have been missed in samples with low IgG levels, especially for AstraZeneca, but also because of the lack of sampling before day 14. In most individuals, afucosylation decreased and reached levels comparable to total IgG three to four weeks after the initial dose. At seroconversion, when anti-S levels are low and neutralizing responses are not yet fully developed, afucosylated anti-S antibodies in naive vaccinees might provide enhanced protection through FcγRIIIa-assisted effector functions.<sup>11,18,50</sup> Subsequently, when these afucosylation levels drop, protection might instead be provided by increased anti-S levels and Fab-mediated neutralizing capacity. Unlike natural SARS-CoV-2 infection, afucosylation upon BNT162b2 vaccination did not correlate with increased IL-6 levels.<sup>12</sup> This disparity might be attributed to the fact that during natural infection, antigen-specific levels coincide with remarkably increased afucosylation, whereas in the context of vaccination, initial levels are low. We observed a sustained decrease in fucosylation after ~50 days for some Janssen vaccinees (7 out of 78), irrespective of a booster dose. Unfortunately, no sampling was performed after day 50–60 for Pfizer, Moderna, and RUMC/COUGH1, which could have facilitated a more thorough comparison. Furthermore, for all vaccine platforms, substantially increased anti-S IgG1 Fc galactosylation and sialylation were observed in comparison to total IgG1 levels, which gradually faded over time, in line with results from other studies.<sup>12,40,52,53</sup> Increased galactosylation enhances the capacity of IgG to form IgG-hexamers and activate complement,<sup>35,38</sup> indicating that enhanced protection through complement might manifest in this early time frame. Overall, the examined vaccine platforms in this study generally seem to mimic the kinetics previously observed in mild SARS-CoV2 infection, namely initial afucosylated and highly galactosylated anti-S IgG1 glycosylation.<sup>18,27,49</sup>

In summary, our data show that vaccination with the S protein delivered by mRNA and adenoviral vectors, both resulting in host-cell membrane expression, as well as S protein-based cVLP vaccine, are capable of eliciting potent antigen-specific IgG antibodies with comparable, but not identical glycoprofiles. These data suggest vaccination induces similar anti-S glycosylation trends in naive individuals, specifically transiently increased galactosylation, sialylation, and decreased fucosylation and bisection. In contrast, total IgG1 glycosylation profiles, slightly influenced by genetic and environmental factors, remained stable and distinct.<sup>31,32,54</sup> Further studies are needed to unravel the mechanism behind this antigen-specific IgG Fc glycosylation and study the influence of both the formulation and timing of re-exposure in the form of a booster. An improved understanding of antigen-specific antibody glycosylation and its underlying mechanism might offer novel routes to improved vaccines but also improved vaccination strategies for enhanced protective immunity.

### Limitations of the study

This work has a number of limitations. One of these is the demographic variation between the different cohorts, as a consequence of being recruited at different times and for distinct purposes. Sex, age, and other demographic characteristics are known to influence total IgG antibody glycosylation. Specifically, total IgG Fc galactosylation and sialylation declines with age and showed significant sex dependence. IgG Fc bisection is known to increase in young adults and reaches a plateau at older age. Conversely, IgG Fc fucosylation is high during early age, but slightly declines throughout adolescence.<sup>11,31,32</sup> In this study, total IgG1 glycosylation was found to be marginally affected by sex and age. A second limitation is the low statistical power to perform potentially meaningful comparisons for Moderna and AstraZeneca due to small sample size that were possible for other cohorts. Besides demographics and sample size, the vaccine cohorts also differed slightly in sample collection timing. The Janssen and RUMC/COUGH1 cohort lacked samples before day 14, and only Janssen included sampling beyond day ~50, making it difficult to formally compare trends in glycosylation patterns for these time points.

### STAR★METHODS

Detailed methods are provided in the online version of this paper and include the following:

- KEY RESOURCES TABLE
- RESOURCE AVAILABILITY
  - Lead contact
  - Materials availability
  - Data and code availability
- EXPERIMENTAL MODEL AND STUDY PARTICIPANTS
  - Ethical statement
  - Human participants
  - Vaccination study cohorts
  - Cell lines
- METHOD DETAILS
  - Anti-SARS-CoV-2 antibody levels
  - IgG Fc glycosylation analysis by mass spectrometry
  - LC-MS data processing
  - FEASI
- QUANTIFICATION AND STATISTICAL ANALYSIS

## SUPPLEMENTAL INFORMATION

Supplemental information can be found online at <https://doi.org/10.1016/j.isci.2023.107619>.

## ACKNOWLEDGMENTS

We thank the Academic Medical Centre of the University of Amsterdam, the Sanquin Blood Supply Foundation, Janssen Vaccines and Prevention B.V., and Radboud University Medical Center (RUMC) & Bavarian Nordic A/S. We furthermore thank all cohort participants, to whom we are greatly indebted for their extensive participation.

Funding: Landsteiner foundation for Blood Transfusion Research (LSBR) grants 1721 and 1908 (G.V.). ZonMW COVID-19 grant 1043001 201 0021 (G.V.). Netherlands Organization for Health Research and Development ZonMw & the Amsterdam UMC Corona Research Fund (Amsterdam UMC COVID-19 S3/HCW study group). The Netherlands Organisation for Health Research and Development ZonMW VENI grant, grant number 09150161910033 (L.A.V.V.). Advancing knowledge for the clinical and public health response to the 2019-nCoV epidemic [H2020-SC1-PHE-CORONAVIRUS-2020 grant agreement ID: 101003608 ] (M.W.). Semper Ardens Carlsberg Foundation (M.W.). This project has been funded in whole or in part with federal funds from the Department of Health and Human Services, Administration for Strategic Preparedness and Response, Biomedical Advanced Research and Development Authority, under Other Transaction Agreement HHSO100201700018C. The findings and conclusions in this report are those of the authors and do not necessarily represent the views of the United States Department of Health and Human Services or its components.

## AUTHOR CONTRIBUTIONS

Conceptualization: G.V., M.W., C.E.v.d.S., A.V., and D.E.S. Methodology: G.V., M.W., J.V.C., T.P., and T.S. Formal analysis: J.V.C., T.P., T.S., and S.K. Investigation: J.V.C., T.S., T.P., S.K., M.S., F.L., R.V., W.W., and J.N. Resources: D.S., L.A.v.V., W.H., M.A.S., R.M., M.K.B., J.J.S., A.S., D.S., M.A.N., B.G.M., R.R., M.L.G., and the UMC COVID-19 S3/HCW study group, Fatebenefratelli-Sacco Infectious Diseases Physicians group and Radboud University Medical Center (RUMC) & Bavarian Nordic (BN) A/S. Data curation: J.V.C., T.S., T.P., S.K., and M.S. Writing – Original draft: G.V., M.W., J.V.C., T.P., and R.R. Writing – Review and editing: J.V.C., T.P., T.S., W.W., J.N., M.L.G., S.K., F.L., O.C., J.B.D.K., R.V., L.A.v.V., M.A.S., N.v.M., M.J.S., A.S., D.E.S., M.S., T.R., M.A.N., B.G.N., A.P.J.V., C.E.v.d.S., R.R., M.W., and G.V. Visualization: T.P. and J.V.C. Supervision: G.V., M.W., A.V., and R.R. Project administration: G.V., M.W., and M.S. Funding acquisition: G.V., M.W., T.P., and Radboud University Medical Center (RUMC) & COUGH1.

## DECLARATION OF INTERESTS

M.L.G. and R.R. are employees of Janssen Pharmaceuticals and M.L.G. is a shareholder in Johnson & Johnson. A.S. and W.A.d.J. are employees at AdaptVac, a company commercializing virus-like particle display technology and vaccines, including several patents. A.S., A.S., T.G.T., and M.N. are founders of AdaptVac and listed as coinventors on a patent covering the AP205 CLP vaccine platform technology (WO2016112921 A1) licensed to AdaptVac. Janssen Pharmaceuticals sponsored IgG glycosylation analysis at LUMC. Sanquin provided consultancy services to Janssen Pharmaceuticals during this study. All other authors declare they have no conflicts of interests.

Received: March 27, 2023

Revised: July 6, 2023

Accepted: August 9, 2023

Published: August 14, 2023

## REFERENCES

1. Adjobimey, T., Meyer, J., Sollberg, L., Bawolt, M., Berens, C., Kovačević, P., Trudić, A., Parcina, M., and Hoerauf, A. (2022). Comparison of IgA, IgG, and Neutralizing Antibody Responses Following Immunization With Moderna, BioNTech, AstraZeneca, Sputnik-V, Johnson and Johnson, and Sinopharm's COVID-19 Vaccines. *Front. Immunol.* **13**, 917905.
2. He, X., Chandrashekar, A., Zahn, R., Wegmann, F., Yu, J., Mercado, N.B., McMahan, K., Martinot, A.J., Piedra-Mora, C., Beecy, S., et al. (2021). Low-dose Ad26.COV2.S protection against SARS-CoV-2 challenge in rhesus macaques. *Cell* **184**, 3467–3473.e11.
3. Solfrosi, L., Kuipers, H., Jongeneelen, M., Rosendahl Huber, S.K., van der Lubbe, J.E.M., Dekking, L., Czapska-Casey, D.N., Izquierdo Gil, A., Baert, M.R.M., Drijver, J., et al. (2021). Immunogenicity and efficacy of one and two doses of Ad26.COV2.S COVID vaccine in adult and aged NHP. *J. Exp. Med.* **218**, e20202756.
4. Mercado, N.B., Zahn, R., Wegmann, F., Loos, C., Chandrashekar, A., Yu, J., Liu, J., Peter, L., McMahan, K., Tostanoski, L.H., et al. (2020). Single-shot Ad26 vaccine protects against SARS-CoV-2 in rhesus macaques. *Nature* **586**, 583–588.
5. Fischer, R.J., van Doremalen, N., Adney, D.R., Yinda, C.K., Port, J.R., Holbrook, M.G., Schulz, J.E., Williamson, B.N., Thomas, T., Barbican, K., et al. (2021). ChAdOx1 nCoV-19 (AZD1222) protects Syrian hamsters against SARS-CoV-2 B.1.351 and B.1.1.7. *Nat. Commun.* **12**, 5868.
6. Gharbharan, A., Jordans, C.C.E., GeurtsvanKessel, C., den Hollander, J.G., Karim, F., Mollema, F.P.N., Stalenhof – Schukken, J.E., Dofferhoff, A., Ludwig, I., Koster, A., et al. (2021). Effects of potent neutralizing antibodies from convalescent plasma in patients hospitalized for severe SARS-CoV-2 infection. *Nat. Commun.* **12**, 3189.
7. Rosenfeld, R., Noy-Porat, T., Mechaly, A., Makdasi, E., Levy, Y., Alcalay, R., Falach, R., Aftalion, M., Epstein, E., Gur, D., et al. (2021). Post-exposure protection of SARS-CoV-2 lethal infected K18-hACE2 transgenic mice by neutralizing human monoclonal antibody. *Nat. Commun.* **12**, 944.
8. Taylor, P.C., Adams, A.C., Hufford, M.M., de la Torre, I., Winthrop, K., and Gottlieb, R.L. (2021). Neutralizing monoclonal antibodies for treatment of COVID-19. *Nat. Rev. Immunol.* **21**, 382–393.
9. Levin, M.J., Ustianowski, A., De Wit, S., Launay, O., Avila, M., Templeton, A., Yuan, Y.,

- Seegobin, S., Ellery, A., Levinson, D.J., et al. (2022). Intramuscular AZD7442 (Tixagevimab-Cilgavimab) for Prevention of Covid-19. *N. Engl. J. Med.* **386**, 2188–2200.
10. Kapur, R., Einarsdottir, H.K., and Vidarsson, G. (2014). IgG-effector functions: “The Good, The Bad and The Ugly”. *Immunol. Lett.* **160**, 139–144.
11. Oosterhoff, J.J., Larsen, M.D., van der Schoot, C.E., and Vidarsson, G. (2022). Afucosylated IgG responses in humans – structural clues to the regulation of humoral immunity. *Trends Immunol.* **43**, 800–814.
12. Van Coillie, J., Pongracz, T., Rahmüller, J., Chen, H.-J., Geyer, C.E., van Vught, L.A., Buhre, J.S., Šuštić, T., van Osch, T.L.J., Steenhuis, M., et al. (2023). The BNT162b2 mRNA SARS-CoV-2 vaccine induces transient afucosylated IgG1 in naive but not in antigen-experienced vaccinees. *EBioMedicine* **87**, 104408.
13. Jansen, B.C., Falck, D., De Haan, N., Hipgrave Ederveen, A.L., Razdorov, G., Lauc, G., and Wührer, M. (2016). LaCyTools: A Targeted Liquid Chromatography-Mass Spectrometry Data Processing Package for Relative Quantitation of Glycopeptides. *J. Proteome Res.* **15**, 2198–2210.
14. Kapur, R., Della Valle, L., Sonneveld, M., Hipgrave Ederveen, A., Visser, R., Ligthart, P., De Haas, M., Wührer, M., van der Schoot, C.E., and Vidarsson, G. (2014). Low anti-RhD IgG-Fc-fucosylation in pregnancy: a new variable predicting severity in haemolytic disease of the fetus and newborn. *bjh* **166**, 936–945.
15. Kapur, R., Kustiawan, I., Vestrheim, A., Koeleman, C.A.M., Visser, R., Einarsdottir, H.K., Porcelijn, L., Jackson, D., Kumpel, B., Andf, A., et al. (2014). A prominent lack of IgG1-Fc fucosylation of platelet alloantibodies in pregnancy. *Blood* **123**, 471–480.
16. Wührer, M., Porcelijn, L., Kapur, R., Koeleman, C.A.M., Deelder, A., de Haas, M., Vidarsson, G., De Haas, M., and Vidarsson, G. (2009). Regulated glycosylation patterns of IgG during alloimmune responses against human platelet antigens. *J. Proteome Res.* **8**, 450–456.
17. Larsen, M.D., Lopez-Perez, M., Dickson, E.K., Ampomah, P., Tuikue Ndam, N., Nouta, J., Koeleman, C.A.M., Ederveen, A.L.H., Mordmüller, B., Salanti, A., et al. (2021). Afucosylated Plasmodium falciparum-specific IgG is induced by infection but not by subunit vaccination. *Nat. Commun.* **12**, 5838.
18. Larsen, M.D., de Graaf, E.L., Sonneveld, M.E., Plomp, H.R., Nouta, J., Hoepel, W., Chen, H.J., Linty, F., Visser, R., Brinkhaus, M., et al. (2021). Afucosylated IgG characterizes enveloped viral responses and correlates with COVID-19 severity. *Science* **371**, eabc8378.
19. Wang, T.T., Sewatanon, J., Memoli, M.J., Wrammert, J., Bournazos, S., Bhaumik, S.K., Pinsky, B.A., Choikephaibulkit, K., Onlamoon, N., Pattanapanyasat, K., et al. (2017). IgG antibodies to dengue enhanced for FcγRIIIA binding determine disease severity. *Science* **355**, 395–398.
20. Ackerman, M.E., Crispin, M., Yu, X., Baruah, K., Boesch, A.W., Harvey, D.J., Dugast, A.S., Heizen, E.L., Ercan, A., Choi, I., et al. (2013). Natural variation in Fc glycosylation of HIV-specific antibodies impacts antiviral activity. *J. Clin. Invest.* **123**, 2183–2192.
21. Bournazos, S., Vo, H.T.M., Duong, V., Auerswald, H., Ly, S., Sakuntabhai, A., Dussart, P., Cantaert, T., Ravetch, J.V., Ly, S., et al. (2021). Antibody fucosylation predicts disease severity in secondary dengue infection. *Science* **372**, 1102–1105.
22. Van Coillie, J., Schulz, M.A., Bentlage, A.E.H., de Haan, N., Ye, Z., Geerdes, D.M., van Esch, W.J.E., Hafkenschied, L., Miller, R.L., Narimatsu, Y., et al. (2022). Role of N-Glycosylation in FcγRIIIa interaction with IgG. *Front. Immunol.* **13**, 1–13.
23. Dekkers, G., Treffers, L., Plomp, R., Bentlage, A.E.H., de Boer, M., Koeleman, C.A.M., Lissenberg-Thunnissen, S.N., Visser, R., Brouwer, M., Mok, J.Y., et al. (2017). Decoding the human immunoglobulin G-glycan repertoire reveals a spectrum of Fc-receptor- and complement-mediated-effector activities. *Front. Immunol.* **8**, 877.
24. Ferrara, C., Grau, S., Jäger, C., Sondermann, P., Brünker, P., Waldhauer, I., Hennig, M., Ruf, A., Rufer, A.C., Stihle, M., et al. (2011). Unique carbohydrate-carbohydrate interactions are required for high affinity binding between FcγRIII and antibodies lacking core fucose. *Proc. Natl. Acad. Sci. USA* **108**, 12669–12674.
25. Temming, A.R., de Taeye, S.W., de Graaf, E.L., de Neef, L.A., Dekkers, G., Bruggeman, C.W., Koers, J., Ligthart, P., Nagelkerke, S.Q., Zimring, J.C., et al. (2019). Functional Attributes of Antibodies, Effector Cells, and Target Cells Affecting NK Cell-Mediated Antibody-Dependent Cellular Cytotoxicity. *J. Immunol.* **203**, 3126–3135.
26. Kapur, R., Della Valle, L., Verhagen, O.J.H.M., Hipgrave Ederveen, A., Ligthart, P., De Haas, M., Kumpel, B., Wührer, M., Van Der Schoot, C.E., and Vidarsson, G. (2015). Prophylactic anti-D preparations display variable decreases in Fc-fucosylation of anti-D. *Transfusion* **55**, 553–562.
27. Pongracz, T., Nouta, J., Wang, W., van Meijgaarden, K.E., Linty, F., Vidarsson, G., Joosten, S.A., M Ottenhoff, T.H., Hokke, C.H., C, J.J., et al. (2021). Immunoglobulin G1 Fc glycosylation as an early hallmark of severe COVID-19. Preprint at medRxiv. <https://doi.org/10.1101/2021.11.18.21266442>.
28. Chakraborty, S., Gonzalez, J., Edwards, K., Mallajosyula, V., Buzzanco, A.S., Sherwood, R., Buffone, C., Kathale, N., Providenza, S., Xie, M.M., et al. (2021). Proinflammatory IgG Fc structures in patients with severe COVID-19. *Nat. Immunol.* **22**, 67–73.
29. Chakraborty, S., Med, S.T., Chakraborty, S., Gonzalez, J.C., Sievers, B.L., Mallajosyula, V., Dubey, M., Ashraf, U., Cheng, B.Y., Kathale, N., et al. (2022). Early Non-neutralizing , Afucosylated Antibody Responses Are Associated with COVID-19 Severity, 7853, pp. 1–20.
30. Farkash, I., Feferman, T., Cohen-Saban, N., Avraham, Y., Morgenstern, D., Mayuni, G., Barth, N., Lustig, Y., Miller, L., Shouval, D.S., et al. (2021). Anti-SARS-CoV-2 antibodies elicited by COVID-19 mRNA vaccine exhibit a unique glycosylation pattern. *Cell Rep.* **37**, 110114.
31. Baković, M.P., Selman, M.H.J., Hoffmann, M., Rudan, I., Campbell, H., Deelder, A.M., Lauc, G., and Wührer, M. (2013). High-throughput IgG Fc N-glycosylation profiling by mass spectrometry of glycopeptides. *J. Proteome Res.* **12**, 821–831.
32. Krištić, J., Vučković, F., Menni, C., Klarić, L., Keser, T., Beceheli, I., Pučić-Baković, M., Novokmet, M., Mangino, M., Thaqi, K., et al. (2014). Glycans Are a Novel Biomarker of Chronological and Biological Ages. *J. Gerontol. A Biol. Sci. Med. Sci.* **69**, 779–789.
33. Gudelj, I., Lauc, G., and Pezer, M. (2018). Immunoglobulin G glycosylation in aging and diseases. *Cell. Immunol.* **333**, 65–79.
34. Peschke, B., Keller, C.W., Weber, P., Quast, I., and Lünemann, J.D. (2017). Fc-Galactosylation of Human Immunoglobulin Gamma Isotypes Improves C1q Binding and Enhances Complement-Dependent Cytotoxicity. *Front. Immunol.* **8**, 646.
35. van Osch, T.L.J., Nouta, J., Derksen, N.I.L., van Mierlo, G., van der Schoot, C.E., Wührer, M., Rispen, T., and Vidarsson, G. (2021). Fc Galactosylation Promotes Hexamerization of Human IgG1, Leading to Enhanced Classical Complement Activation. *J. Immunol.* **207**, 1545–1554.
36. Van Osch, T.L.J., Oosterhoff, J.J., Bentlage, A.E.H., Nouta, J., Koeleman, C.A.M., Geerdes, D.M., Mok, J.Y., Heidt, S., Mulder, A., Van Esch, W.J.E., et al. (2022). Fc Galactosylation of Anti-platelet IgG1 Alloantibodies Enhance Complement Activation on Platelets. *Haematologica* **107**, 2432–2444.
37. Diebold, C.A., Beurskens, F.J., de Jong, R.N., Koning, R.I., Strumane, K., Lindorfer, M.A., Voorhorst, M., Ugurlar, D., Rosati, S., Heck, A.J.R., et al. (2014). Complement is activated by IgG hexamers assembled at the cell surface. *Science* **343**, 1260–1263.
38. Wei, B., Gao, X., Cadang, L., Izadi, S., Liu, P., Zhang, H.M., Hecht, E., Shim, J., Magill, G., Pabon, J.R., et al. (2021). Fc galactosylation follows consecutive reaction kinetics and enhances immunoglobulin G hexamerization for complement activation. *mAbs* **13**, 1893427.
39. Temming, A.R., Dekkers, G., Van De Bovenkamp, F.S., Plomp, H.R., Bentlage, A.E.H., Sztittner, Z., Derksen, N.I.L., Wührer, M., Rispen, T., and Vidarsson, G. (2019). Human DC-SIGN and CD23 do not interact with human IgG. *Sci. Rep.* **9**, 9995.
40. Selman, M.H.J., De Jong, S.E., Soonawala, D., Kroon, F.P., Adegnika, A.A., Deelder, A.M., Hokke, C.H., Yazdanbakhsh, M., and Wührer, M. (2012). Changes in antigen-specific IgG1 Fc N-glycosylation upon influenza and tetanus vaccination. *Mol. Cell. Proteomics* **11**, M111.014563.
41. van Erp, E.A., Lakerveld, A.J., de Graaf, E., Larsen, M.D., Schepp, R.M., Hipgrave Ederveen, A.L., Ahout, I.M., de Haan, C.A., Wührer, M., Luytjens, W., et al. (2020). Natural killer cell activation by respiratory syncytial virus-specific antibodies is decreased in infants with severe respiratory infections and correlates with Fc-glycosylation. *Clin. Transl. Immunol.* **9**, e1112.
42. Alter, G., Ottenhoff, T.H.M., and Joosten, S.A. (2018). Antibody glycosylation in inflammation, disease and vaccination. *Semin. Immunol.* **39**, 102–110.
43. Smit, M.J., Sander, A.F., Ariaans, M.B.P.A., Fougereux, C., Heinzl, C., Fendel, R., Esen, M., Kremsner, P.G., ter Heine, R., Wertheim, H.F., et al. (2023). First-in-human use of a modular capsid virus-like vaccine platform: an open-label, non-randomised, phase 1 clinical trial of the SARS-CoV-2 vaccine ABNCoV2. *Lancet Microbe* **4**, e140–e148.
44. Šuštić, T., Van Coillie, J., Larsen, M.D., Derksen, N.I.L., Sztittner, Z., Nouta, J., Wang, W., Damelang, T., Bergegen, I., Linty, F., et al. (2022). Immunoassay for quantification of antigen-specific IgG fucosylation. *EBioMedicine* **81**, 104109.
45. Roozendaal, R., Solfarosi, L., Stieh, D.J., Serroyen, J., Straetmans, R., Dari, A.,

- Boulton, M., Wegmann, F., Rosendahl Huber, S.K., M van der Lubbe, J.E., et al. SARS-CoV-2 Binding and Neutralizing Antibody Levels after Ad26.COV2.S Vaccination Predict Durable Protection in Rhesus Macaques
46. Wall, E.C., Wu, M., Harvey, R., Kelly, G., Warchal, S., Sawyer, C., Daniels, R., Adams, L., Hobson, P., Hatipoglu, E., et al. (2021). AZD1222-induced neutralising antibody activity against SARS-CoV-2 Delta VOC. *Lancet* **398**, 207–209.
  47. Pongracz, T., Vidarsson, G., and Wuhrer, M. (2022). Antibody glycosylation in COVID-19. *Glycoconj. J.* **39**, 335–344.
  48. Siekman, S.L., Pongracz, T., Wang, W., Nouta, J., Kramsner, P.G., Silva-neto, P.V., Esen, M., Trape, A., Kreidenweiss, A., Held, J., et al. (2022). The IgG Glycome of SARS-CoV-2 Infected Individuals Reflects Disease Course and Severity.
  49. Chakraborty, S., Edwards, K., Buzzanco, A.S., Memoli, M.J., Mallajosyula, V., Xie, M.M., Gonzalez, J., Buffone, C., Providenza, S., Jagannathan, P., et al. (2020). Symptomatic SARS-CoV-2 infections display specific IgG Fc structures. Preprint at medRxiv. <https://doi.org/10.1101/2020.05.15.20103341>.
  50. Hoepfel, W., Chen, H.-J., Geyer, C.E., Allahverdiyeva, S., Manz, X.D., de Taeye, S.W., Aman, J., Mes, L., Steenhuis, M., Griffith, G.R., et al. (2021). High titers and low fucosylation of early human anti-SARS-CoV-2 IgG promote inflammation by alveolar macrophages. *Sci. Transl. Med.* **13**, eabf8654.
  51. Matrose, N.A., Obikese, K., Belay, Z.A., and Caleb, O.J. (2019). Anti-SARS-CoV-2 antibodies elicited by COVID-19 mRNA vaccine exhibit a unique glycosylation pattern. *Sci. Total Environ.* **135907**.
  52. Vestrheim, A.C., Moen, A., Egge-Jacobsen, W., Reubsaet, L., Halvorsen, T.G., Bratlie, D.B., Paulsen, B.S., and Michaelsen, T.E. (2014). A pilot study showing differences in glycosylation patterns of IgG subclasses induced by pneumococcal, meningococcal, and two types of influenza vaccines. *Inflamm. Dis.* **2**, 76–91.
  53. Wang, T.T., Maamary, J., Tan, G.S., Bourmazos, S., Davis, C.W., Krammer, F., Schlesinger, S.J., Palese, P., Ahmed, R., and Ravetch, J.V. (2015). Anti-HA Glycoforms Drive B Cell Affinity Selection and Determine Influenza Vaccine Efficacy. *Cell* **162**, 160–169.
  54. De Haan, N., Reiding, K.R., Driessen, G., Van Der Burg, M., and Wuhrer, M. (2016). Changes in healthy human IgG Fc-glycosylation after birth and during early childhood. *J. Proteome Res.* **15**, 1853–1861.
  55. Steenhuis, M., van Mierlo, G., Derksen, N.I., Ooijevaar-de Heer, P., Kruithof, S., Loeff, F.L., Berkhout, L.C., Linty, F., Reusken, C., Reimerink, J., et al. (2021). Dynamics of antibodies to SARS-CoV-2 in convalescent plasma donors. *Clin. Transl. Immunol.* **10**, e1285.
  56. Pongracz, T., Nouta, J., Wang, W., Van Meijgaarden, K.E., Linty, F., Vidarsson, G., Joosten, S.A., Ottenhoff, T.H.M., Hokke, C.H., De Vries, J.J.C., et al. (2022). Immunoglobulin G1 Fc glycosylation as an early hallmark of severe COVID-19. *EBioMedicine* **78**, 103957.
  57. Brouwer, P.J.M., Caniels, T.G., van der Straten, K., Snitselaar, J.L., Aldon, Y., Bangaru, S., Torres, J.L., Okba, N.M.A., Claireaux, M., Kerster, G., et al. (2020). Potent neutralizing antibodies from COVID-19 patients define multiple targets of vulnerability. *Science* **369**, 643–650.
  58. Pucić, M., Knezević, A., Vidic, J., Adamczyk, B., Novokmet, M., Polasek, O., Gornik, O., Supraha-Goreta, S., Wormald, M.R., Redžić, I., et al. (2011). High throughput isolation and glycosylation analysis of IgG-variability and heritability of the IgG glycome in three isolated human populations. *Mol. Cell. Proteomics* **10**, M111.010090.

STAR★METHODS

KEY RESOURCES TABLE

REAGENT or RESOURCE	SOURCE	IDENTIFIER
<b>Antibodies</b>		
anti-IgG HRP	Sanquin	M1268
streptavidin–poly-HRP	Sanquin	M2032
<b>Biological samples</b>		
Vaccinee sera	Amsterdam University Medical Center and Janssen Vaccines and Prevention B.V.	S3 cohort; NL 73478.029.20, Netherlands Trial Register NL8645, and
<b>Chemicals, peptides, and recombinant proteins</b>		
Spike protein	In house	Brouwer et al.
Nucleocapsid protein	In house	Brouwer et al.
FcγRIIIa-V158	In house	Šuštić et al.
TMB	Thermo Scientific	#34029
Tween 20	Sigma Aldrich	Cat# P9416-100ML
BirA	Sanquin	N/A
Sequencing Grade Modified Trypsin	Promega	Cat#V511A
Formic Acid	Sigma-Aldrich	Cat#94318; CAS: 64-18-6
Acetonitrile (LC-MS grade)	Biosolve	Cat#012078; CAS: 75-05-
Trifluoroacetic Acid (LC-MS grade)	Merck	Cat#85183; CAS: 76-05-1
Ammonium Bicarbonate	Sigma-Aldrich	Cat#09830; CAS: 1066-33
<b>Critical commercial assays</b>		
Anti-S IgG Abs level measurement	Nexelis	N/A
Anti-N IgG Abs level measurement	Nexelis	N/A
<b>Deposited data</b>		
Liquid chromatography - Mass spectrometry data	This paper, deposited in MassIVE dataset Repository	<a href="https://doi.org/10.25345/C59P2WG9B">https://doi.org/10.25345/C59P2WG9B</a> Accession code: MSV000092012
<b>Experimental models: Cell lines</b>		
293T	ATCC	CRL-1573
<b>Software and algorithms</b>		
LaCyTools	Jansen et al.	<a href="https://git.lumc.nl/cpm/lacyttools">https://git.lumc.nl/cpm/lacyttools</a>
R	R Foundation for Statistical Computing	<a href="https://www.r-project.org/">https://www.r-project.org/</a>
RStudio	Posit Software, PBC	<a href="https://posit.co/">https://posit.co/</a>
Bruker Compass DataAnalysis	Bruker Daltonics	<a href="https://www.bruker.com/">https://www.bruker.com/</a>
MSConvertGUI	ProteoWizard	<a href="https://proteowizard.sourceforge.io/">https://proteowizard.sourceforge.io/</a>
<b>Other</b>		
NUNC MaxiSorp 96-well flat-bottom plates	Sigma Aldrich	M9410
Corning 3690 half-area plates	Sigma Aldrich	CLS3690
Protein G AssayMAP Cartridge	Agilent	G5496-60008
HisTRAP column	Sigma Aldrich	GE17-5255-01

## RESOURCE AVAILABILITY

### Lead contact

Further information and requests for resources and reagents should be directed to and will be fulfilled by the lead contact, Prof. Gestur Vidarsson ([g.vidarsson@sanquin.nl](mailto:g.vidarsson@sanquin.nl)).

### Materials availability

The vaccinee sera is a limited resource.

### Data and code availability

- The Liquid chromatography - Mass spectrometry data generated for this study is available at <https://doi.org/10.25345/C59P2WG9B> (Accession code: MSV000092012).
- The code used to generate the visualizations in this study are available from T. Pongracz upon reasonable request.
- Any additional information required to reanalyze the data reported in this paper is available from the [lead contact](#) upon request.

## EXPERIMENTAL MODEL AND STUDY PARTICIPANTS

### Ethical statement

All participants were included through informed written consent and all studies complied with the latest version of the Declaration of Helsinki.

### Human participants

All vaccinee participants were included through informed written consent and all studies complied with the latest version of the Declaration of Helsinki. All available demographic information is reported in [Tables S1–S5](#). An analysis on the influence of sex and gender on the results is reported in [Tables S6–S8](#). Formal sample size calculations were not conducted for this current study, nor were individuals included based on demographics, i.e. samples were included based on availability.

### Vaccination study cohorts

#### *Cohort 1. Pfizer*

Subjects were part of the S3 cohort study (S3 cohort; NL 73478.029.20, Netherlands Trial Register NL8645), a prospective serologic surveillance cohort study among hospital healthcare workers in the Amsterdam University Medical Center (Amsterdam UMC). Between January and March 2021, 39 cohort participants received their first dose of BNT162b2 mRNA vaccine (Pfizer/BioNTech). A second dose was administered approximately 21 days after the first dose. Samples were obtained directly before (pre-vaccination) and around 3, 7, 10 and 14 days after the first dose, and directly before and around 3, 7, 10, 14, 21 and 28 days after the second dose. The ethics committee of the AUMC approved the study. Furthermore, nine healthcare workers at the Luigi Sacco Infectious Diseases Hospital, Milano, Italy were included in this cohort. They received a 2<sup>nd</sup> dose 21 days after the 1<sup>st</sup> dose. Blood samples were obtained directly before the 1<sup>st</sup> dose, and twice a week for six weeks from December 2020 to February 2021 ([Tables 1](#) and [S1](#)). All participants were included through informed written consent.

#### *Cohort 2. Moderna*

This cohort is part of the S3 cohort study (S3 cohort; NL 73478.029.20, Netherlands Trial Register NL8645), a prospective serologic surveillance cohort study among hospital healthcare workers in the Amsterdam University Medical Center (Amsterdam UMC). On April 9<sup>th</sup> of 2021, a cohort of healthcare workers (n=8) received their first dose of the SpikeVax mRNA vaccine (Moderna). The second dose was administered 28 days after the first. Samples were obtained directly before (pre-vaccination) and 3, 7, 10 and 14 days after the first vaccination, and directly before and 3, 7, 10, 14, 21 and 28 days after the second dose ([Tables 1](#) and [S2](#)). Six individuals had both anti-N and anti-S levels above threshold prior to vaccination, of which 5 had a positive PCR test. The ethics committee of the AUMC approved the study.

#### *Cohort 3. Janssen*

This cohort is part of the Janssen Vaccines and Prevention B.V. VAC31518COV2001 clinical trial. Participants (n=75) received the JCOVDEN adenovirus-based vaccine. A second dose was administered to 38 of the participants after 57 days after the first dose. Samples were obtained on the day of vaccination (pre-vaccination) and 15, 29, 57, 64, 71, 85, and 169 days after the first dose ([Tables 1](#) and [S3](#)). Based on anti-N ELISA results, it was concluded that five volunteers may have had antigen experience with SARS-CoV-2 prior to study enrolment. While anti-N positivity of these volunteers was above cut-off (100-130 AU; cut-off: 48 AU) at each of the three sampling points (day 1, 57, 169), only one volunteer had anti-S levels (192 AU) above cut-off (50 AU) at day 1. For none of these volunteers anti-S IgG1 glycosylation profiling could be determined. Thus, as four of these volunteers were negative based on both anti-S ELISA and MS following affinity-isolation of anti-S antibodies, the results suggest that the anti-N ELISA readouts were false positives. Based on these assumptions, it was concluded that only one volunteer was antigen-experienced at baseline. Anti-N data further suggested that two volunteers possibly became infected during the study, as the first volunteer was positive for the N antigen at day 169 (454 AU), and volunteer two at day 59 (304 AU) and day 169 (317 AU). Two volunteers



showed anti-N ELISA levels just above cut-off: for the first volunteer day 1 (50 AU) and day 57 (57 AU) and for the second at day 1 (56 AU). Again, none of these volunteers were anti-S positive using neither by anti-S ELISA nor by MS at day 1, indicating potential false positivity. Lastly, one volunteer was considered as a non-responder, because at none of the time points did (s)he show anti-S positivity by ELISA.

#### Cohort 4. AstraZeneca

This cohort is part of the S3 cohort study (S3 cohort; NL 73478.029.20, Netherlands Trial Register NL8645), a prospective serologic surveillance cohort study among hospital healthcare workers in the Amsterdam University Medical Center (Amsterdam UMC). Between April 7<sup>th</sup> and 15<sup>th</sup> 2021, a cohort of healthcare workers (n=17) received their first dose of the ChAdOx1 nCoV-19 adenovirus-based vaccine (AstraZeneca). The criteria for this vaccine were based on their age of 60 years or older, as part of the national vaccination strategy in the Netherlands. A second dose was administered 6 to 10 weeks after the first dose. Samples were obtained directly before (pre-vaccination) and approximately 3, 7, 10, 14, 21 and 28 days after the first dose, and directly before and 3, 7, 10, 14, 21 and 28 days after the second dose (Tables 1 and S4). The ethics committee of the AUMC approved the study.

#### Cohort 5. RUMC/COUGH1

This cohort is part of the NCT04839146 clinical trial of Radboud University Medical Center (RUMC) in the framework of the EU-funded Prevent-nCoV project to evaluate the immunogenicity, safety, and tolerability of ABNCoV2 vaccine in SARS-CoV-2 seronegative and seropositive adult subjects.<sup>43</sup> Participants (n=45) were included in seven different regimens and received different ABNCoV2 protein vaccine (RBD domain) concentrations with and without MF59 adjuvants. A second dose was received around 26-35 days after the first dose. Samples were obtained around 14 and 25 days after the first dose and 14 days after the second dose (Tables 1 and S5).

#### Cell lines

HEK 293 cells (human embryonic kidney cell: ATCC, CRL-3216) were maintained at 37°C in Dulbecco's modified Eagle's Medium (DMEM, Sigma-Aldrich, Cat# D6429) supplemented with 10% heat-inactivated fetal bovine serum (FBS, Sigma-Aldrich).

## METHOD DETAILS

### Anti-SARS-CoV-2 antibody levels

For the Pfizer, Moderna, AstraZeneca and RUMC/COUGH1 cohort, anti-S IgG and -N total Abs levels were measured by anti-S IgG ELISA and anti-N bridging ELISA, respectively.<sup>12,44,55</sup> The spike and nucleocapsid protein containing a polyhistidine and BirA tag were produced in-house in HEK 293 cells. Washing steps in either ELISA included five washes with PBS supplemented with 0.02% polysorbate-20 (PBS-T), after every step described below other than stopping development. Samples in either ELISA were diluted in PBS-T supplemented with 0.3% gelatin (PTG). Absorbance was measured at 450 and 540 nm, and the difference was used for further analysis (optical density, OD).

The anti-S IgG ELISA was performed in MaxiSorp microplates (Thermo Fisher Scientific) with a per-step volume of 100 µg/well. Plates were coated overnight at 4°C with 1 µg/ml S in PBS. Samples were diluted 1:400 to 1:1200 in PTG depending on the anti-S IgG levels and incubated for 1 hour at room temperature (RT) while shaking. 0.5 µg/ml anti-IgG HRP (Sanquin, MH16-1) in PTG was then incubated for 30 minutes at RT while shaking. Lastly, 75% tetramethylbenzidine substrate (TMB, Thermo, 34029, 25% water) was added to develop, and the reaction was stopped with 0.2 M H<sub>2</sub>SO<sub>4</sub> (Merck). Anti-S IgG levels were determined based on a pooled plasma standard collected from COVID-19 convalescent healthy donors in May 2020, arbitrarily assigned a value of 100 AU/ml and used in a 1:1 serial dilution from 1:400 to 1:25600 with a PTG blank.

The anti-N bridging ELISA was performed in half-area microplates (Corning 3690) with a per-step volume of 50 µg/well. Plates were coated overnight at 4°C with 0.3 µg/ml N in PBS. Samples were diluted 1:10 in PTG and incubated for 1 hour at RT while shaking. 0.008 µg/ml in-house biotinylated N in PTG was incubated for 1 hour at RT while shaking, followed by incubation with 1:10 000 streptavidin-poly-HRP (Sanquin, M2032) in PTG for 30 min at RT while shaking. 75% tetramethylbenzidine substrate (TMB, Thermo, 34029, 25% water) was added to develop, and the reaction was stopped with 0.2 M H<sub>2</sub>SO<sub>4</sub> (Merck). OD values were normalized to readings of the same May 2020 plasma pool described above, which was included on each plate, and reported as normalized OD (nOD).

The anti-S IgG levels of 264 pre-pandemic samples were determined and the pre-outbreak threshold of 3.19 AU/ml for seropositivity was determined based on the 95<sup>th</sup> percentile of these samples.

Anti-S and -N IgG Abs level measurements for the Janssen cohort were carried out at Nexelis (Laval, Canada) using their validated ELISA.<sup>45</sup>

### IgG Fc glycosylation analysis by mass spectrometry

Anti-S IgG Abs were affinity-captured.<sup>12,18,56</sup> NUNC MaxiSorp 96-well flat-bottom plates (Sigma Aldrich) were coated with 250 µl/well in-house produced, trimerized, spike protein-coated plates at 5 µg/ml in PBS at 4°C overnight.<sup>18,57</sup> Plates were washed five times in PBST and incubated with 200 µl/well 1:10 diluted plasma or serum in PBS for 1 hour at RT, shaking. Plates were washed five times in PBST, followed by a 200 µl/well 100 mM formic acid elution step.

Total IgG Abs were affinity-captured from plasma or sera using 5 µl Protein G AssayMAP Cartridge Rack on the Bravo (Agilent Technologies).<sup>12,18</sup> For this, 0.5 µl serum or plasma diluted in 100 µl PBS was applied to the cartridges, followed by washes with PBS and LC-MS grade water. IgG antibodies were eluted with 40 µl 1% formic acid.

Eluates from both anti-S and total IgG affinity-purification were dried by vacuum centrifugation and subjected to tryptic digestion overnight at 37°C following their resuspension in 20 µl 50 mM ammonium bicarbonate and 20 µl sequencing grade trypsin solution (25 ng per sample; Promega Corporation, WI, Madison). Following tryptic digestion, the purified anti-S IgG glycopeptides were either measured directly or stored at -20°C until LC-MS analysis.<sup>12,18,27</sup>

Glycopeptides were separated and detected using an Dionex Ultimate 3000 high-performance liquid chromatography (HPLC) system (Thermo Fisher Scientific, Waltham, MA) equipped with an PepMap™ Neo C18 (5 µm particles, 100 Å pores, 0.3 x 5 mm) (Thermo Fisher Scientific, cat. nr. 174500) and NanoEase M/Z peptide BEH C18 (1.7 µm particles, 130 Å pores, 75 µm x 100 mm) (Waters, cat. no. 186008792) analytical column. First, five hundred nL of total IgG or two hundred nL of anti-S IgG was injected into the system, followed by loading on the trap column at a flowrate of 25 µl/min of eluent A (0.02% TFA) for 1 min at 45°C for pre-concentration and desalting purposes. After valve switching, the glycopeptides were backflushed toward the analytical column, and separated with a two-step linear gradient from 97% solvent A (0.02% trifluoroacetic acid in water) and 3% solvent B (95% ACN) down to 21.7% solvent B in 4.5 min, after which it goes to 50% within a minute (5.5 min), at a flowrate of 600 nL/min at 45°C. The LC system was hyphenated to an Impact HD quadrupole time-of-flight mass spectrometer (Bruker Daltonics, Billerica, MA) via an electrospray ionization interface, which was equipped with a CaptiveSpray nanoBooster using ACN-enriched nitrogen gas (at 0.2 bar pressure and a dry gas flow rate of 3 l/min). A frequency of 1 Hz was used for recording the spectra in the m/z range of 550–1800 in positive ion polarity mode. The transfer time was set to 110 ms, the pre-pulse storage time to 21 µs, while the collision energy was set to 5 eV. This method allowed unambiguous identification of IgG Fc glycopeptides in a subclass-specific manner based on accurate mass (MS1) and specific migration positions in liquid chromatography.

### LC-MS data processing

Liquid chromatography-mass spectrometry data processing mzXML files were generated from raw liquid chromatography - mass spectrometry (LC-MS) spectra. Raw LC-MS spectra were analysed using the in-house developed software LaCyTools.<sup>13</sup> LC-MS readouts that had no corresponding anti-S ELISA result were excluded. Alignment was performed based on average retention time of at least three highly abundant glycoforms. The analyte list for targeted extraction of the 2<sup>+</sup> and 3<sup>+</sup> charge states was based on manual annotation as well as on literature reports<sup>18,58</sup> and inclusion of an analyte was based on quality criteria as follows: a signal-to-noise higher than 9, isotopic pattern quality less than 25% deviation from the theoretical isotopic pattern, and mass error within a ±20 parts per million range (Table S9). For reasons of comparability, an overlapping glycopeptides list was used to calculate glycosylation traits (bisection, galactosylation, sialylation and fucosylation) by normalizing the relative intensity of each glycopeptide species to the sum of their total areas (Table S10), analogously to previous reports.<sup>12,18,27</sup> All analytes in the overlapping glycopeptide list conformed with the described quality criteria.

### FEASI

Fucose-sensitive ELISA for antigen-specific IgG was performed as described in Šuštić et al.<sup>44</sup> Human FcγRIIIa-V158 containing a polyhistidine tag and Avi-Tag was cloned in the pcDNA3.1 mammalian expression vector. The receptor was produced in HEK293 Freestyle cells and five days after transfection, the supernatants was harvested, filtered and isolated using a HIS-trap column (GE Life Sciences) on an ÄKTA prime plus system (GE Life Sciences). The receptor was site-specific C-terminally biotinylated. For biotinylation of 1 µM FcγRIIIa, 3.3 nM BirA ligase (Sanquin) was added and MWCO 10 kDa Amicon Ultra centrifugal filter units (Merck, Millipore) were used to concentrate the sample and remove unbound biotin.

Spike-specific IgG from each plasma and/or serum sample was captured on in-house produced spike protein-coated NUNC MaxiSorp 96-well flat-bottom plates (Sigma Aldrich). For this, plates were coated overnight with 100 µl/well 1 µg/ml recombinant spike protein in PBS. Plates were washed five times with PBST and incubated for 1 hour with 100 µl/well of a dilution range of serum or plasma samples in PTG, depending on the anti-S IgG levels. After incubation, plates were washed five times with PBST. For the FcγR-ELISA, 100 µl/well 1 µg/ml biotinylated FcγRIIIa in PBST was added for 1 hour, washed five times in PBST, and incubated with 100 µl/well 0.1 µg/ml streptavidin-poly-HRP (Sanquin, M2032) in PBST and washed five times in PBST. For the IgG-ELISA, plates were incubated with 100 µl/well 1 µg/ml anti-human IgG HRP in PBST (Sanquin, M1268) and washed five times in PBST. Both ELISA's were developed with 100 µl/well 50% water-diluted tetramethylbenzidine substrate (1-step ultra TMB, Thermo Scientific, #34029). Absorbance was measured at 450 and 540 nm and reported as optical density (OD).

Serial dilutions of each plasma and/or serum sample were compared to the convalescent blood donors plasma pool and assigned a value of 100 arbitrary units, which corresponds approximately to 21 µg/ml.<sup>44,55</sup> Logit log transformation of serial dilutions of this calibrator sample was used as a standard curve to calculate AU values for each dilution of each sample. The geometric mean of AU values from each individual serial dilution was taken as an AU value representative of the particular sample. Ratios of AU values between the FcγRIIIa-IgG and the IgG ELISA were calculated for each assay, and geometric mean of ratios calculated from two or more independent replicates was used to calculate anti-spike fucosylation percentage according to the simple linear regression established in Šuštić et al.<sup>44</sup> and defined as  $y = -0.096x + 9.893$ . Geometric mean of AU values from the IgG ELISA replicates were used to represent the abundance of anti-spike IgG in each sample. Detection threshold was set at 0.469 AU and quantification threshold was based on the 95<sup>th</sup> percentile of signals of 264 pre-outbreak plasma samples, as previously defined.<sup>55</sup>

### QUANTIFICATION AND STATISTICAL ANALYSIS

Cohorts' demographics were compared by ANOVA followed by Tukey's post-hoc test (age) (Table S6) and Chi-squared test (sex). To compare anti-S IgG levels (Figure S4) and relative abundances of anti-S (Figure S6) and total IgG1 Fc glycosylation traits (Figure S8), Kruskal-Wallis tests were carried out. In case of significance, a Kruskal-Wallis test was followed by post-hoc Dunn's test(s) (Figures S4, S6, and S8). For the comparison of paired groups, a Wilcoxon signed-rank test was used (Figures S1 and S7). Spearman's correlation was used to explore correlations between IgG(1) Fc fucosylation measured by FEASI and MS (Figure 4), as well as to investigate correlations between demographics and anti-S IgG levels, or anti-S and total IgG1 Fc glycosylation (Tables S7 and S8). *P*-values < 0.05 were considered as significant following correction for multiple testing per statistical question using the Benjamini-Hochberg procedure with a false discovery rate (FDR) of 5%. Asterisks indicate the degree of significance as follows: \*, \*\*, \*\*\*, \*\*\*\*: *p*-value < 0.05, 0.01, 0.001, 0.0001, respectively. Statistical analyses and visualizations were performed in R (version 4.2.2; R foundation for Statistical Computing, Vienna, Austria) and RStudio (version 2022.12.0, Build 353; RStudio, Boston, MA).